THE JOURNAL OF BIOLOGICAL CHEMISTRY VOL. 289, NO. 38, pp. 26302–26313, September 19, 2014

Insulin Receptor Substrate-4 Binds to Slingshot-1 Phosphatase and Promotes Cofilin Dephosphorylation*

Received for publication, March 15, 2014, and in revised form, August 3, 2014 Published, JBC Papers in Press, August 6, 2014, DOI 10.1074/jbc.M114.565945

Yuta Homma[‡], Shin-ichiro Kanno[§], Kazutaka Sasaki[‡1], Michiru Nishita[‡2], Akira Yasui[§], Tomoichiro Asano[¶], Kazumasa Ohashi[‡], and Kensaku Mizuno[‡3]

From the [‡]Department of Biomolecular Sciences, Graduate School of Life Sciences, Tohoku University, Sendai, Miyagi 980-8578, Japan, [§]Division of Dynamic Proteome in Cancer and Aging, Institute of Development, Aging and Cancer, Tohoku University, Sendai, Miyagi 980-8575, Japan, and [¶]Department of Medical Science, Graduate School of Medicine, University of Hiroshima, Hiroshima, Hiroshima 734-8553, Japan

Background: Slingshot-1 is a cofilin phosphatase that dephosphorylates and activates actin filament-severing activity of cofilin.
Results: Insulin receptor substrate-4 (IRS4) binds to and co-localizes with Slingshot-1 and promotes cofilin dephosphorylation.
Conclusion: IRS4 promotes local activation of cofilin via binding to Slingshot-1 and activation of phosphatidylinositol 3-kinase.
Significance: Our findings indicate a novel function of IRS4 in Slingshot-1 activation and actin dynamics.

Cofilin plays an essential role in cell migration and morphogenesis by enhancing actin filament dynamics via its actin filament-severing activity. Slingshot-1 (SSH1) is a protein phosphatase that plays a crucial role in regulating actin dynamics by dephosphorylating and reactivating cofilin. In this study, we identified insulin receptor substrate (IRS)-4 as a novel SSH1-binding protein. Co-precipitation assays revealed the direct endogenous binding of IRS4 to SSH1. IRS4, but not IRS1 or IRS2, was bound to SSH1. IRS4 was bound to SSH1 mainly through the unique region (amino acids 335–400) adjacent to the C terminus of the phosphotyrosine-binding domain of IRS4. The N-terminal A, B, and phosphatase domains of SSH1 were bound to IRS4 independently. Whereas *in vitro* phosphatase assays revealed that IRS4 does not directly affect the cofilin phosphatase activity of SSH1, knockdown of IRS4 increased cofilin phosphorylation in cultured cells. Knockdown of IRS4 decreased phosphatidylinositol 3-kinase (PI3K) activity, and treatment with an inhibitor of PI3K increased cofilin phosphorylation. Akt preferentially phosphorylated SSH1 at Thr-826, but expression of a non-phosphorylatable T826A mutant of SSH1 did not affect insulin-induced cofilin dephosphorylation, and an inhibitor of Akt did not increase cofilin phosphorylation. These results suggest that IRS4 promotes cofilin dephosphorylation through sequential activation of PI3K and SSH1 but not through Akt. In addition, IRS4 co-localized with SSH1 in F-actin-rich membrane protrusions in insulin-stimulated cells, which suggests that the association of IRS4 with SSH1 contributes to localized activation of cofilin in membrane protrusions.

Actin filament dynamics and reorganization play essential roles in various cellular events, including cell migration, division, polarity formation, and vesicle transport. Actin dynamics are spatially and temporally regulated by a large number of actin-binding proteins. Cofilin is an actin-binding protein that promotes actin assembly/disassembly dynamics through its severing activity in actin filaments (1). Cofilin is inactivated by phosphorylation of Ser-3 by LIM kinase and testicular protein kinase (2–5). Ser-3-phosphorylated cofilin (P-cofilin)[4] is dephosphorylated and reactivated by the Slingshot (SSH) family of protein phosphatases (6, 7) and chronophin (8). Therefore, these kinases and phosphatases play crucial roles in regulating actin dynamics through cofilin inactivation and activation, respectively (5). *SSH* was initially identified as one of the causal genes for malformation of bristles in *Drosophila* (6). Three *SSH* genes (*SSH1*, *SSH2*, and *SSH3*) exist in the human and mouse genomes (5–7). Human *SSH1* gene is transcribed and translated to several isoforms, including a long isoform (SSH1L) and a short isoform (SSH1S), by alternative splicing (6). In mammalian cells, SSH1 is activated in response to a variety of extracellular stimuli, including neuregulin, insulin, stromal cell-derived factor-1, and calcium ionophore (9–12). The cofilin phosphatase activity of SSH1 is dramatically increased by binding to F-actin (9, 13). SSH1 accumulates on the F-actin-rich lamellipodium, which probably contributes to the local activation of cofilin and rapid turnover of actin filaments at the leading edge of the migrating cell (9, 11). In chemokine-stimulated cells, depletion of SSH1 results in the formation of multiple lamellipodia and impairs chemotactic migration (11), indicating that SSH1 is an important regulator that mediates stimulus-induced actin remodeling to induce polarized cellular migration. SSH1 is activated downstream of phosphatidylinositol 3-kinase (PI3K) (10). Although SSH2 was shown to be activated downstream of the PI3K-Akt-GSK3 signaling pathway

* This work was supported by Grants for Scientific Research 24121702 and 24370051 (to K. M.) from the Ministry of Education, Culture, Science, Sports and Technology of Japan.
[1] Present address: Shiseido Research Center, Yokohama 224-8558, Japan.
[2] Present address: Dept. of Physiology and Cell Biology, Graduate School of Medicine, Kobe University, Kobe 650-0017, Japan.
[3] To whom correspondence should be addressed. Tel.: 81-22-795-6676; Fax: 81-22-795-6678; E-mail: kmizuno@biology.tohoku.ac.jp.

[4] The abbreviations used are: P-cofilin, Ser-3-phosphorylated cofilin; CFP, cyan fluorescent protein; GSK3, glycogen synthase kinase 3; IRS, insulin receptor substrate; P-Akt, phosphorylated Akt; P-GSK3α/β, phosphorylated GSK3α/β; sr, shRNA-resistant; SSH, Slingshot; SSH1L, long isoform of SSH1; SSH1S, short isoform of SSH1; PH, pleckstrin homology; PTB, phosphotyrosine-binding; PDK, 3-phosphoinositide-dependent protein kinase; mTOR, mammalian target of rapamycin.

(14), it remains unknown whether SSH1 is similarly activated via the Akt-GSK3 pathway. Furthermore, the molecular mechanisms by which SSHs are localized in the lamellipodium are not fully understood (5).

The insulin receptor substrate (IRS) family proteins consist of IRS1, IRS2, IRS3, and IRS4 isoforms. Of these, IRS3 is absent in primates. They act as scaffolding proteins to mediate insulin signaling (15). IRS proteins contain a pleckstrin homology (PH) domain and a phosphotyrosine-binding (PTB) domain in the N-terminal region, which is followed by a long, non-conserved C-terminal tail that has numerous tyrosine and serine phosphorylation sites. Upon insulin stimulation, tyrosine residues in NP*XY* motifs of insulin receptors are autophosphorylated, which is followed by the binding of the PTB domain of IRSs to phosphorylated tyrosine residues of insulin receptors, and then several tyrosine residues of the Y*XX*M motifs in the C-terminal region of IRSs are phosphorylated by insulin receptors. IRSs then recruit and activate the Src homology-2 domain-containing proteins, such as PI3K, triggering an increase in the levels of phosphatidylinositol 3,4,5-trisphosphate and activation of a variety of downstream protein kinases, such as PDK1, PDK2, Akt, PKCζ, and mTOR (15). Thus, IRS proteins mediate insulin and other growth factor signaling from the upstream tyrosine kinase receptors to the downstream signaling pathways.

In this study, we identified IRS4 as a novel SSH1-binding protein. We provide evidence that IRS4, but not IRS1 or IRS2, interacts with SSH1 through the medial region that is not conserved between the IRS family proteins. IRS4 binds to SSH1 endogenously and co-localizes with SSH1 in membrane protrusions. Our results suggest that IRS4 promotes cofilin dephosphorylation via activation of PI3K but not Akt and that the IRS4-SSH1 interaction contributes to localized activation of cofilin in membrane protrusions.

EXPERIMENTAL PROCEDURES

Reagents and Antibodies—Insulin was purchased from Sigma (I5523). LY294002 and Akt inhibitor VIII were purchased from Merck (440202 and 124018). SB216763 was purchased from Sigma (S3442). His_6-tagged active recombinant Akt1 was purchased from Merck. Antibodies against cofilin, P-cofilin, and SSH1L were prepared as described previously (4, 16). Other antibodies used in this study were: GFP (Molecular Probes, A6455), Myc (Roche Applied Science, 9E10), FLAG (Sigma, M2), IRS4 (Abcam, ab52622), Akt1 (Cell Signaling Technology, 2H10), P-Akt (Thr-308) (Cell Signaling Technology, 9275), P-Akt (Ser-473) (Cell Signaling Technology, 4051 and 9271), phospho-Akt substrate (Cell Signaling Technology, 9611), GSK3α/β (Santa Cruz Biotechnology, sc-7291), P-GSK3α/β (Cell Signaling Technology, 9331), β-catenin (BD Biosciences, 610153), Alexa Fluor 488-labeled anti-rabbit IgG (Molecular Probes, A11034), and Alexa Fluor 568-labeled anti-mouse IgG (Molecular Probes, A11031). Alexa Fluor 568-labeled phalloidin was purchased from Molecular Probes (A12380).

Plasmid Construction—FPC1-Myc vector was constructed by replacing the GFP-coding sequence of pEGFP-C1 (Clontech) with the Myc tag-coding sequence. The pFastBac1-GST vector was constructed by inserting the glutathione *S*-transferase (GST)-coding sequence at the 5′ terminus to the multiple cloning site of pFastBac1 (Invitrogen). The pFastBac1-GST-FLAG vector was constructed by inserting the FLAG-coding sequence at the 5′ terminus to the multiple cloning site of pFastBac-GST vector. Human IRS4 cDNA (FHC27470) was purchased from Kazusa DNA Research Institute (Kisarazu, Chiba, Japan). The PCR-amplified cDNA fragments of full-length and deletion mutants of IRS4 were subcloned into pEYFP-C1 (Clontech), FPC1-Myc, and pFastBac1-GST vectors. Full-length SSH1L was subcloned into a pFastBac-GST-FLAG vector. Full-length SSH1L or SSH1S was subcloned into a pcDNA5/FRT/TO vector (Invitrogen). Other cDNA constructs of SSH1L mutants were prepared as described previously (13). The cDNA plasmids for Myc-tagged IRS1 and IRS2 were constructed as described previously (17). The short hairpin RNA (shRNA) expression plasmids were constructed by inserting two independent target sequences against human IRS4 into pSUPER vector (Oligoengine). The shRNA target sequences were as follows: shIRS4-2 (5′-GCTGTATGGATATTCTCT-3′), shIRS4-3 (5′-GTTTCAACCTGTTGCTAAT-3′), and control shGL2 (5′-CCGTACGCGGAATACTTCGA-3′). The shRNA-resistant (sr), yellow fluorescent protein (YFP)-tagged IRS4 (sr-YFP-IRS4) cDNA was constructed by introducing silent mutations into a target sequence of shIRS4-2 (GTTGCATGGACATCTCCCT; mutated nucleotides are underlined) using a QuikChange site-directed mutagenesis kit (Stratagene).

Cell Culture and Transfection—The 293T cells were cultured in Dulbecco's modified Eagle's medium supplemented with 10% fetal calf serum, 40 μg/ml streptomycin, and 40 units/ml penicillin. Plasmids were transfected into 293T cells using FuGENE HD (Roche Applied Science) following the manufacturer's instructions.

Proteomic Analysis—The 293T cell lines that inducibly express FLAG-tagged SSH1L or SSH1S were established using the Flp-In T-REx 293 cell line system (Invitrogen) according to the manufacturer's instruction. To induce expression, cells were treated with doxycycline (final concentration, 1 μg/ml) for 48 h. Cells were then sonicated in lysis buffer (50 mM HEPES, pH 7.5, 0.3 M NaCl, 0.5% Nonidet P-40) supplemented with protease inhibitors (Roche Applied Science). Cell lysates were immunoprecipitated with an anti-FLAG M2 affinity column (Sigma). The precipitated proteins were eluted with lysis buffer containing 100 μg/ml FLAG peptide (Sigma), separated by SDS-PAGE, and stained using a silver stain kit (Wako). Protein bands were excised from the gels, reduced by 100 mM dithiothreitol (DTT), and alkylated with 100 mM iodoacetamide. After washing, the gels were incubated with trypsin for 10 h at 30 °C. Recovered peptides were desalted by ZipTip C_{18} (Millipore) and analyzed using a nano-liquid chromatography-tandem mass spectrometry (LC/MS/MS) system (DiNA HPLC system, KYA Technologies Corp./QSTAR XL, Applied Biosystems) as described previously (18). Mass data acquisition was piloted through Mascot software by Japan Proteomics.

Co-immunoprecipitation Assay—The 293T cells were harvested 24 h after transfection. Cells were lysed in lysis buffer (50 mM Tris-HCl, pH 7.5, 1% Triton X-100, 10% glycerol, 150 mM NaCl, 50 mM NaF, 1 mM Na_3VO_4, 10 μg/ml leupeptin, 1 mM DTT) and centrifuged at 15,000 rpm for 10 min. The supernatants were precleared by incubation with Protein A-Sepharose

4 Fast Flow (GE Healthcare) for 1 h at 4 °C and then centrifuged at 15,000 rpm for 10 min. The supernatants were incubated with an appropriate antibody and Protein A-Sepharose 4 Fast Flow for 2 h at 4 °C. The beads were washed with wash buffer (50 mM Tris-HCl, pH 7.5, 1% Triton X-100, 10% glycerol, 300 mM NaCl, 50 mM NaF, 1 mM Na_3VO_4, 10 μg/ml leupeptin, 1 mM DTT) three times and boiled in sample buffer (62.5 mM Tris-HCl, pH 6.8, 5% 2-mercaptoethanol, 2% SDS, 5% sucrose, 0.005% bromphenol blue). Samples were subjected to SDS-PAGE and analyzed by immunoblotting using an appropriate antibody.

Protein Purification—FLAG-SSH1L was purified by using the following procedure. GST-FLAG-SSH1 was expressed in Sf21 cells using the Bac-to-Bac baculovirus expression system (Invitrogen). Cells were sonicated in lysis buffer and clarified by centrifugation. The supernatants were incubated with glutathione-Sepharose 4B (GE Healthcare) for 2 h. After washing with buffer (50 mM Tris-HCl, pH 7.5, 150 mM NaCl, 1 mM DTT, 0.1% Triton X-100), the beads were incubated in this buffer with Prescission protease (GE Healthcare) to remove the GST tag. Eluted proteins were applied to a PD-10 column (GE Healthcare) equilibrated with buffer (50 mM Tris-HCl, pH 7.5, 1% Triton X-100, 150 mM NaCl, 1 mM DTT). GST and GST-IRS4 were expressed in Sf21 cells and purified using glutathione-Sepharose 4B as described above. After washing with buffer (50 mM Tris-HCl, pH 7.5, 150 mM NaCl, 0.1% Triton X-100), GST and GST-IRS4 were eluted with the buffer supplemented with 30 mM glutathione and applied to a PD-10 column equilibrated with buffer (50 mM Tris-HCl, pH 7.5, 1% Triton X-100, 150 mM NaCl, 1 mM DTT). GST tags were removed by Prescission protease to obtain non-tagged IRS4 for *in vitro* phosphatase assays. Cofilin-His_6 was expressed in 239T cells and purified with nickel-nitrilotriacetic acid-agarose as described previously (13). Eluted cofilin-His_6 was dialyzed against Tris buffer (25 mM Tris-HCl, pH 7.5, 100 mM NaCl, 1 mM DTT).

In Vitro Binding Assay—GST or GST-IRS4 was immobilized on glutathione-Sepharose 4B. The beads were incubated in 600 μl of lysis buffer with FLAG-SSH1L at 4 °C for 1 h. The beads were washed three times with lysis buffer and boiled in sample buffer. Samples were analyzed by immunoblotting using an anti-FLAG antibody.

In Vitro Phosphatase Assay—Purified FLAG-SSH1L and cofilin-His_6 were incubated together in 20 μl of buffer (50 mM Tris-HCl, pH 7.5, 100 mM NaCl, 2 mM $MgCl_2$, 1 mM DTT) at 30 °C for 1 h in the presence or absence of purified IRS4. The 4× sample buffer was added to stop the reaction, and the samples were analyzed by immunoblotting using an anti-P-cofilin antibody.

In Vitro Kinase Assay—SSH1L-Myc or its mutants were expressed in 293T cells, immunoprecipitated with anti-Myc antibody, and incubated with 400 ng of His_6-tagged recombinant active Akt and 1 mM ATP in kinase reaction buffer (50 mM HEPES, pH 7.4, 150 mM NaCl, 1 mM $MgCl_2$, 1 mM $MnCl_2$, 20 mM NaF, 1 mM Na_3VO_4, 1 mM DTT) for 1 h at 30 °C. Reaction mixtures were analyzed by immunoblotting using an anti-phospho-Akt substrate antibody.

IRS4 Knockdown and Rescue Experiments—The 293T cells were plated on a 6-well dish at 1.0×10^5 cells/well. For knockdown experiments, cells were transfected with shRNA plasmids and cultured for 48 h. For rescue experiments, cells were co-transfected with shGL2 or shIRS4-2 in combination with YFP or sr-YFP-IRS4 and cultured for 48 h. Media were changed to serum-free media and cultured for 2 h before the cells were harvested with sample buffer. Total cell lysates were boiled for 15 min and analyzed by immunoblotting using antibodies against P-cofilin, cofilin, P-Akt, Akt, and IRS4.

Immunoblotting—Denatured proteins were resolved by SDS-PAGE and transferred to polyvinylidene difluoride membranes. The membranes were blocked with skimmed milk and incubated with appropriate antibodies. Horseradish peroxidase-conjugated anti-rabbit or -mouse IgG antibody was used as the secondary antibody.

Immunofluorescence Staining—The 293T cells were plated on poly-L-lysine-coated coverslips in 35-mm dishes. Cells were fixed with 4% paraformaldehyde at 37 °C for 15 min, permeabilized with 0.1% Triton X-100 for 5 min, and blocked with 2% fetal calf serum. Cells were then incubated with appropriate antibodies. Alexa Fluor 488-labeled anti-rabbit IgG antibody and Alexa Fluor 568-labeled anti-mouse IgG antibody were used as secondary antibodies. Alexa Fluor 568-phalloidin was used for F-actin staining. Fluorescent images were obtained using an inverted fluorescence microscope (Leica, DMI6000 B) equipped with a Plan-Apochromat 63× oil immersion objective lens and a cooled charge-coupled device camera (Roper Scientific, CoolSNAP HQ).

Statistical Analysis—Data are expressed as the means ± S.E. An unpaired *t* test was used to assess significant differences between two groups. Significance levels were adjusted with a Bonferroni correction, and they are indicated in the figure legends.

RESULTS

Identification of IRS4 as an SSH1-binding Protein—Human *SSH1* gene has two splice variants, SSH1L (1049 amino acids) and SSH1S (692 amino acids; Fig. 1*A*) (6). To examine the regulatory mechanisms of SSH1, we searched SSH1-binding proteins by proteomic analysis. The 293T cell lines expressing either FLAG-tagged SSH1L or SSH1S were established, and the cell lysates were immunoprecipitated with an anti-FLAG antibody. The co-precipitated proteins were separated by SDS-PAGE, silver-stained, and analyzed by mass spectrometric analysis (Fig. 1*A*). IRS4 was identified in SSH1S co-precipitates. To examine whether IRS4 specifically binds to SSH1S or binds to both SSH1S and SSH1L, YFP or YFP-tagged IRS4 was co-expressed with Myc-tagged SSH1L or SSH1S in 293T cells and immunoprecipitated with an anti-GFP antibody, and the precipitates were analyzed by anti-Myc immunoblotting. Both Myc-SSH1L and -SSH1S were co-precipitated with YFP-IRS4 but not with YFP (Fig. 1*B*), indicating that IRS4 binds to both SSH1L and SSH1S. SSH1S appeared to have a higher affinity to IRS4 than SSH1L. However, the expression of endogenous SSH1S was hardly detected in 293T cells. Therefore, we focused on the interaction between SSH1L and IRS4.

To examine whether IRS4 associates with SSH1L endogenously, cell lysates of 293T cells were immunoprecipitated with an anti-SSH1L antibody or control IgG, and the precipitates

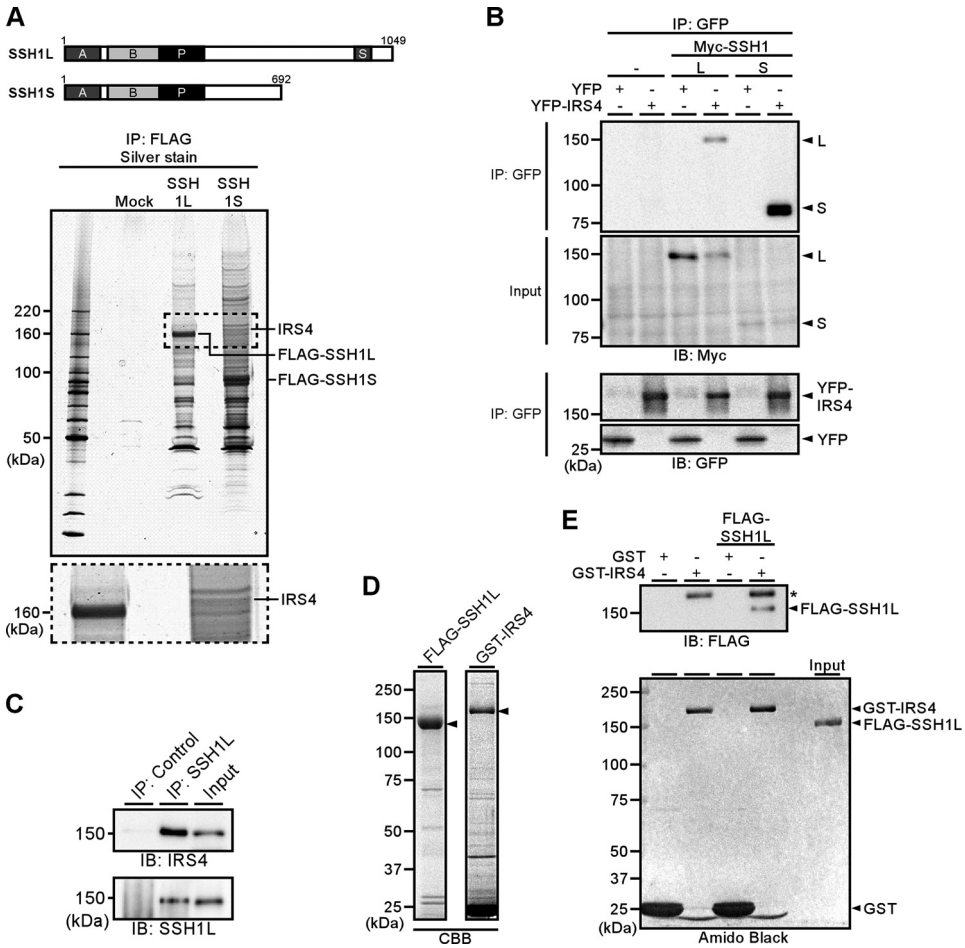

FIGURE 1. **SSH1 interacts with IRS4 in cultured cells and *in vitro*.** *A*, identification of SSH1-binding proteins. The 293T cell lines stably expressing FLAG-SSH1L or -SSH1S were established, and cell lysates were precipitated with an anti-FLAG antibody. The co-precipitated proteins were separated by SDS-PAGE, stained by silver, and analyzed by mass spectrometric analysis. The magnified image of the *dashed box* region is shown at the bottom. *B*, IRS4 interacts with both SSH1L (*L*) and SSH1S (*S*). The 293T cells were co-expressed with YFP-IRS4 and Myc-SSH1L or -SSH1S. Cell lysates were immunoprecipitated (*IP*) with an anti-GFP antibody and analyzed by immunoblotting (*IB*) with anti-Myc and anti-GFP antibodies. *C*, IRS4 interacts with SSH1L endogenously. The 293T cell lysates were immunoprecipitated with an anti-SSH1L antibody or control IgG and analyzed by immunoblotting with anti-SSH1L and anti-IRS4 antibodies. *D*, purity of FLAG-SSH1L and GST-IRS4. FLAG-SSH1L and GST-IRS4 were expressed in Sf21 cells, purified, and subjected to SDS-PAGE. The gel was stained with Coomassie Brilliant Blue (*CBB*). *E*, IRS4 directly interacts with SSH1L *in vitro*. GST or GST-IRS4 was immobilized on glutathione-Sepharose beads and incubated with FLAG-SSH1L. The beads were washed, and the precipitates were analyzed by immunoblotting using an anti-FLAG antibody. GST and GST-IRS4 were visualized by Amido Black staining. The *asterisk* indicates the position of the nonspecific signals probably due to the presence of a large amount of GST-IRS4 proteins in the precipitates.

were analyzed by immunoblotting with an anti-IRS4 antibody. Endogenous IRS4 was detected in the immunoprecipitates with an anti-SSH1L antibody but not with control IgG (Fig. 1*C*). These results indicate that IRS4 and SSH1L associate endogenously in 293T cells.

To examine whether SSH1L directly binds to IRS4, an *in vitro* binding assay was performed using purified proteins. FLAG-SSH1L and GST-IRS4 were expressed in Sf21 cells by a baculovirus expression system and purified (Fig. 1*D*). When the purified FLAG-SSH1L was incubated with GST or GST-IRS4 immobilized on glutathione-Sepharose, FLAG-SSH1L was bound to GST-IRS4 but not control GST (Fig. 1*E*), indicating that SSH1L directly binds to IRS4.

Mapping of SSH1L-binding Region of IRS4—IRS family proteins, including IRS1, IRS2, and IRS4, have the highly conserved PH and PTB domains in their N-terminal regions. To determine which region of IRS4 is involved in its binding to SSH1L, the individual Myc-tagged deletion mutants of IRS4 (shown in Fig. 2*A*) were co-expressed with cyan fluorescent protein (CFP)-tagged SSH1L in 293T cells, and their binding ability was analyzed by immunoprecipitation with an anti-GFP antibody followed by immunoblotting with an anti-Myc antibody. Serial truncations of IRS4 from the C terminus to amino acid residue 401 did not affect the SSH1L binding ability (Fig. 2*B*). Moreover, neither the deletion of the PH domain (amino acids 200–1257) nor the deletion of both PH and PTB domains (amino acids 335–1257) affected the binding ability of IRS4 to SSH1L (Fig. 2*B*). IRS4(1–400), IRS4(200–400), and IRS4(335–400) were bound to SSH1L, but IRS4(1–334) did not bind (Fig. 2*C*), indicating that region 335–400 adjacent to the C terminus of the PTB domain is necessary and sufficient for IRS4 to bind to SSH1L. IRS4(401–1257) had weak SSH1L binding ability, but IRS4(401–1093) did not bind (Fig. 2*D*). Together, these results suggest that region 335–400 is the major SSH1L-binding region of IRS4, and the C-terminal region 1094–1257 has an additional weak binding ability. The regions 335–400 and

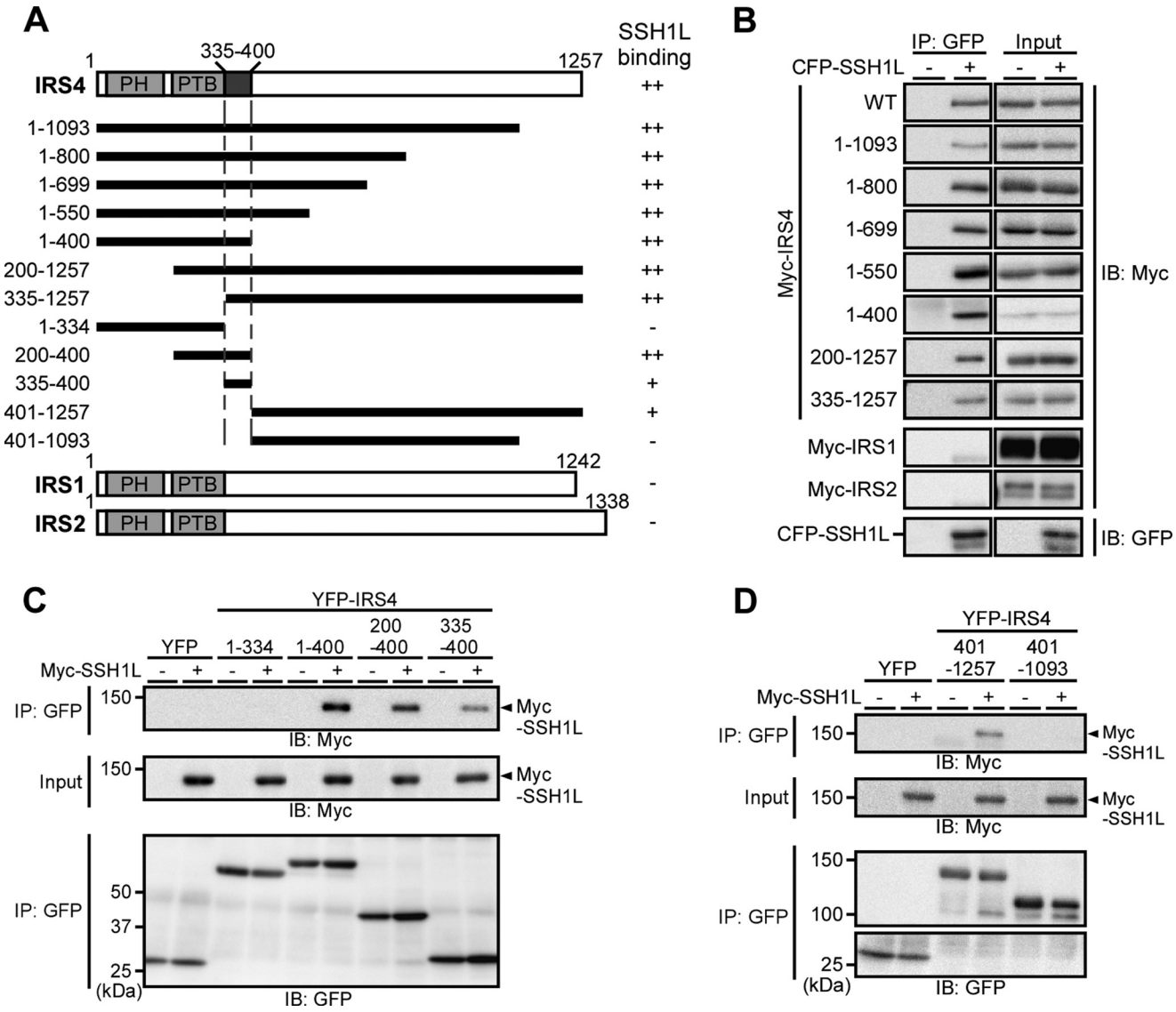

FIGURE 2. **Mapping of SSH1L-binding regions of IRS4.** *A*, schematic structure of human IRS4 and its deletion mutants used in this study. *PH* and *PTB* indicate the PH and the PTB domains. A major SSH1L-binding region (amino acids 335–400) is indicated. The SSH1L binding ability of each construct is indicated in the *right column*. *B–D*, co-immunoprecipitation assays. *B*, 293T cells co-expressing CFP-SSH1L and Myc-IRS4 or its mutants, Myc-IRS1, or -IRS2 were lysed and immunoprecipitated with an anti-GFP antibody. Immunoprecipitates (*IP*) and cell lysates (*Input*) were analyzed by immunoblotting (*IB*) with anti-Myc or anti-GFP antibody. *C* and *D*, 293T cells co-expressing Myc-SSH1L and YFP-IRS4 mutants were lysed and immunoprecipitated with an anti-GFP antibody. Immunoprecipitates and cell lysates were analyzed by immunoblotting with anti-Myc or anti-GFP antibody.

1094–1257 of IRS4 have no sequence similarity to the corresponding regions of IRS1 and IRS2. Consequently, IRS1 and IRS2 did not bind to SSH1L (Fig. 2*B*).

Mapping of IRS4-binding Region of SSH1L—To map the IRS4-binding region of SSH1L, CFP-tagged wild-type (WT) SSH1L and its deletion mutants (shown in Fig. 3*A*) were co-expressed with Myc-IRS4 or Myc-IRS4(1–400) in 293T cells and immunoprecipitated with an anti-GFP antibody, and the precipitates were analyzed by immunoblotting with an anti-Myc antibody. Myc-IRS4 was co-immunoprecipitated with CFP-SSH1L(WT) and CFP-SSH1L(N461) (Fig. 3*B*), indicating that IRS4 binds to the N-terminal region of SSH1L. SSH1L(N461) contains the functional domains consisting of the A domain (a domain required for F-actin-mediated activation of SSH1L), the B domain (a domain involved in P-cofilin recognition and F-actin binding), and the P domain (a phosphatase catalytic domain) (13). Co-immunoprecipitation assays revealed that Myc-IRS4(1–400) binds to each of the A, B, and P domains independently (Fig. 3*C*). Myc-IRS4(1–400) was bound to BP and AP fragments but not to the AB fragment (Fig. 3*C*).

Knockdown of IRS4 Increases Cofilin Phosphorylation in Cultured Cells—To explore the role of IRS4 in the regulation of SSH1 activity in cultured cells, we analyzed the effect of IRS4 knockdown on the level of cofilin phosphorylation in 293T cells. Two independent shRNA plasmids (shIRS4-2 and -3) targeting human IRS4 were constructed. Cells were transfected with each of the shRNA plasmids and cultured for 48 h, and the level of cofilin phosphorylation was assessed by immunoblotting using an anti-P-cofilin antibody. Immunoblot analysis revealed that transfection of each of the IRS4 shRNAs effectively suppressed the expression of endogenous IRS4 protein in 293T cells (Fig. 4*A*). Transfection of each IRS4 shRNA signifi-

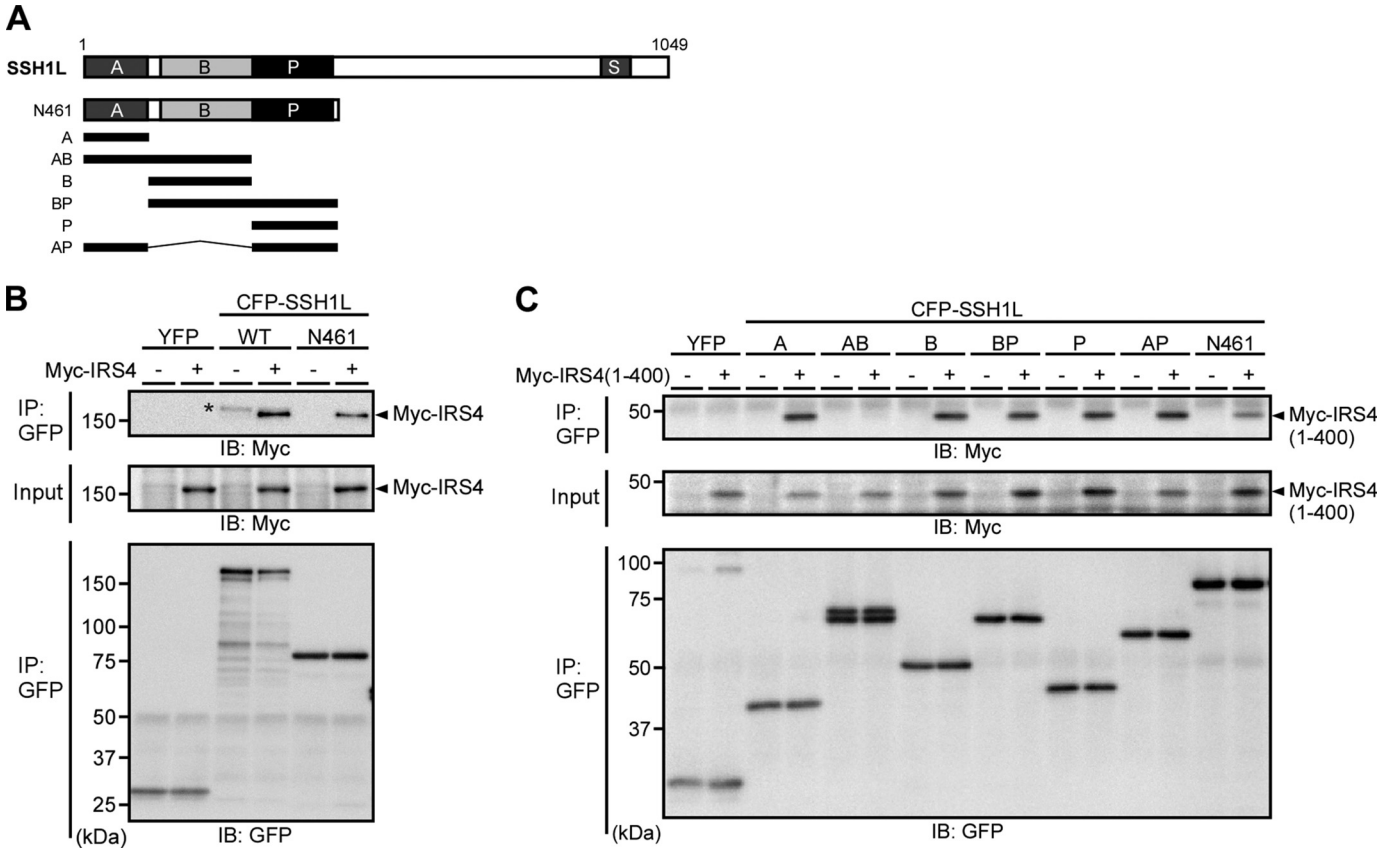

FIGURE 3. **Mapping of IRS4-binding regions of SSH1L.** *A*, schematic structure of human SSH1L and its deletion mutants used in this study. The conserved regions in the SSH family are indicated by the A, B, P (phosphatase), and S (serine-rich) domains. *B* and *C*, co-immunoprecipitation assays. The 293T cells co-expressing CFP-SSH1L or its mutants and Myc-IRS4 or its fragment (amino acids 1–400) were lysed and immunoprecipitated with an anti-GFP antibody. Immunoprecipitates (*IP*) and cell lysates (*Input*) were analyzed by immunoblotting (*IB*) with anti-Myc or anti-GFP antibody. The *asterisk* in *B* indicates the nonspecific signal probably derived from CFP-SSH1L in the precipitates.

cantly increased the level of cofilin phosphorylation compared with that of control shRNA but did not affect the level of total cofilin (Fig. 4*A*), which suggests that endogenous IRS4 functions to promote cofilin dephosphorylation. To further examine the role of IRS4 in cofilin dephosphorylation, we analyzed the effect of expression of sr-YFP-IRS4 on the increase in P-cofilin levels induced by IRS4 shRNA. Exogenous expression of sr-YFP-IRS4 was detected by immunoblot analysis using an anti-IRS4 antibody (Fig. 4*B*). Expression of sr-YFP-IRS4 reduced the level of P-cofilin, and the increase in P-cofilin levels induced by IRS4 shRNA was significantly reduced to the levels in control shRNA cells (Fig. 4*B*). These results suggest that the effect of IRS4 shRNA is caused by depletion of IRS4 and that endogenous IRS4 promotes cofilin dephosphorylation in cultured cells.

IRS4 Has No Direct Effect on Cofilin Phosphatase Activity of SSH1L—Because IRS4 induces cofilin dephosphorylation in cultured cells and it directly binds to SSH1L, we examined whether IRS4 directly promotes cofilin phosphatase activity of SSH1L. To test this possibility, an *in vitro* phosphatase assay was performed using purified FLAG-SSH1L, cofilin-His_6, and IRS4. Cofilin-His_6 was expressed in 293T cells, purified, and used as a substrate. FLAG-SSH1L and IRS4 were expressed in Sf21 cells by a baculovirus expression system and purified (Fig. 1*D*). FLAG-SSH1L was incubated at 30 °C for 60 min with cofilin-His_6 in the presence or absence of IRS4, and the reaction mixtures were analyzed by immunoblotting using an anti-P-cofilin antibody. FLAG-SSH1L dephosphorylated P-cofilin, but addition of almost equal amounts of IRS4 had no apparent effect on the cofilin phosphatase activity of SSH1L (Fig. 5), suggesting that IRS4 binding does not directly promote cofilin phosphatase activity of SSH1L.

IRS4 Activates the PI3K-Akt Pathway in Cultured Cells—We showed previously that SSH1L is activated downstream of PI3K (10). To examine the possibility that IRS4 activates SSH1L through PI3K activation, we analyzed the effect of IRS4 knockdown on PI3K activity. Activation of PI3K was assessed by immunoblot analysis of Thr-308/Ser-473-phosphorylated Akt (P-Akt), a protein kinase that is activated downstream of PI3K. Knockdown of IRS4 by shRNAs markedly decreased the levels of P-Akt (Thr-308) and P-Akt (Ser-473) without affecting the levels of total Akt in 293T cells (Fig. 4, *A* and *C*). The decrease in the P-Akt (Thr-308) and P-Akt (Ser-473) levels by IRS4 knockdown was reversed by exogenous expression of sr-YFP-IRS4 (Fig. 4, *B* and *D*, *lanes 3* and *4*). These results suggest that IRS4 promotes PI3K activation. In addition, we assessed Akt activity by analyzing the levels of phosphorylated GSK3α and GSK3β (P-GSK3α and P-GSK3β), which are downstream targets of Akt. Knockdown of IRS4 decreased the levels of P-GSK3α and -3β without affecting the levels of total GSK3α and -3β (Fig. 4*C*), and the decrease in the levels of P-GSK3α/-3β by IRS4 knockdown was recovered by exogenous expression of sr-YFP-

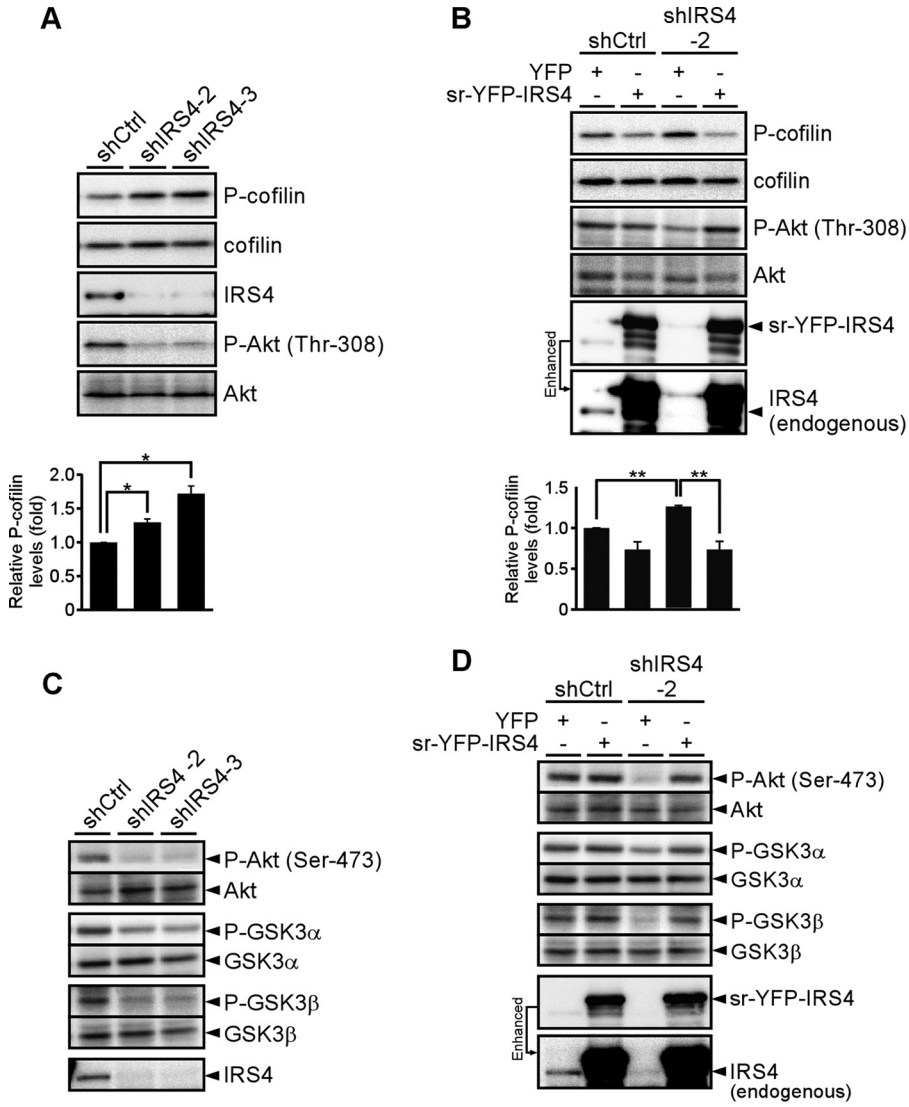

FIGURE 4. **Knockdown of IRS4 increases cofilin phosphorylation, and overexpression of IRS4 reverses the level of cofilin phosphorylation in IRS4-depleted cells.** *A* and *C*, effects of IRS4 knockdown on the levels of phosphorylation of cofilin, Akt, GSK3α, and GSK3β. The 293T cells were transfected with control GL2 shRNA (*shCtrl*) or shRNAs targeting IRS4 (shIRS4-2 and -3) and cultured for 48 h. Cell lysates were analyzed by immunoblotting with antibodies against IRS4, cofilin, P-cofilin, Akt, P-Akt (Thr-308), P-Akt (Ser-473), GSK3α, GSK3β, and P-GSK3α/β. Quantification of the P-cofilin/cofilin ratio is shown in the *bottom graph* in *A*. Data are the means ± S.E. (*error bars*) ($n = 4$; unpaired *t* tests with Bonferroni correction). *, $p < 0.025$. *B* and *D*, rescue experiments of IRS4 knockdown cells. The 293T cells were transfected with shCtrl or shIRS4-2 in combination with YFP or sr-YFP-IRS4 and cultured for 48 h. Expression of sr-YFP-IRS4 and endogenous IRS4 was analyzed by immunoblotting with an anti-IRS4 antibody. The levels of protein phosphorylation were analyzed as in *A* and *C*. Quantification of the P-cofilin/cofilin ratio is shown in the *bottom graph* in *B*. Data are the means ± S.E. (*error bars*) ($n = 5$; unpaired *t* tests with Bonferroni correction). **, $p < 0.005$.

IRS4 (Fig. 4*D*). These results suggest that IRS4 promotes activation of PI3K and Akt.

A PI3K Inhibitor, but Not an Akt Inhibitor, Increases Cofilin Phosphorylation—A previous study showed that SSH2 is activated downstream of the PI3K-Akt-GSK3 pathway (14). To examine the role of this pathway in SSH1L activation, we analyzed the effects of pharmacological inhibitors of PI3K, Akt, and GSK3 on the levels of cofilin phosphorylation in 293T cells. Inhibition of PI3K by treatment with LY294002 increased the level of cofilin phosphorylation compared with that in control cells (Fig. 6*A*), suggesting that PI3K has a critical role in promoting cofilin dephosphorylation. Treatment with LY294002 decreased the levels of P-Akt (Ser-473), P-GSK3α, and P-GSK3β without affecting the levels of total Akt, GSK3α, and -3β (Fig. 6*A*), indicating that PI3K promotes activation of Akt. We next examined the effects of an Akt inhibitor, Akt VIII, on the level of cofilin phosphorylation. Intriguingly, inhibition of Akt by Akt VIII treatment decreased the levels of cofilin phosphorylation (Fig. 6*A*), which suggests that, in contrast to PI3K, Akt has an inhibitory role in cofilin dephosphorylation. Treatment with Akt VIII decreased the levels of P-Akt (Ser-473) and P-GSK3α/-3β (Fig. 6*A*), indicating that Akt VIII inhibited Akt activity. Inhibition of GSK3α/-3β by SB216763 did not affect the level of cofilin phosphorylation. Together, these results suggest that SSH1L is activated downstream of PI3K but not through the Akt-GSK3 pathway.

Akt Preferentially Phosphorylates SSH1L at Thr-826, but This Phosphorylation Has No Effect on Insulin-induced Cofilin Dephosphorylation—To further examine the role of Akt in regulating SSH1L activity, we analyzed whether Akt phosphory-

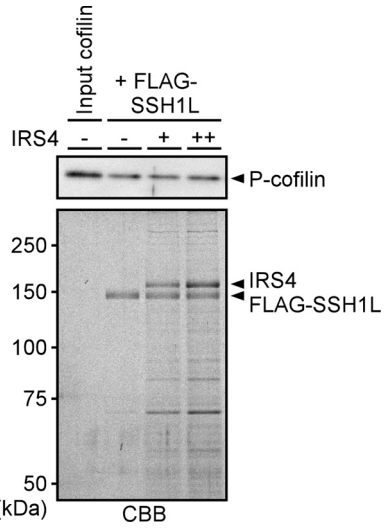

FIGURE 5. **IRS4 has no direct effect on cofilin phosphatase activity of SSH1L.** Purified FLAG-SSH1L was incubated with cofilin-His_6 at 30 °C for 1 h in the presence or absence of purified IRS4. SDS sample buffer was added to stop the reaction. Reaction mixtures were subjected to SDS-PAGE and analyzed by immunoblotting using an anti-P-cofilin antibody. FLAG-SSH1L and IRS4 were analyzed by Coomassie Brilliant Blue (*CBB*) staining.

lates SSH1L. SSH1L-Myc was immunoprecipitated with an anti-Myc antibody, incubated with active Akt protein, and analyzed by immunoblotting with an anti-phospho-Akt substrate antibody that recognizes R*XX*(pS/pT) where pS is phosphoserine and pT is phosphothreonine. This analysis revealed that active Akt phosphorylates SSH1L(WT)-Myc and its phosphatase-dead (C393S) mutant, in which the catalytic residue Cys-393 was replaced by Ser (Fig. 6*B*). *In vitro* kinase assays using a set of C-terminally truncated mutants of SSH1L-Myc revealed that active Akt effectively phosphorylates SSH1L(1–896) and SSH1L(1–830) but only weakly phosphorylates SSH1L(1–807) and shorter fragments, indicating that Akt predominantly phosphorylates the region of amino acids 808–830 of SSH1L (Fig. 6*C*). Because this region contains the $RKHT^{826}$ sequence, we constructed a T826A mutant of SSH1L in which Thr-826 was replaced by alanine. *In vitro* kinase assays revealed that active Akt effectively phosphorylates SSH1L(WT) but only faintly phosphorylates SSH1L(T826A) (Fig. 6*D*), indicating that Thr-826 is the major phosphorylation site of SSH1L by Akt.

To examine the role of Thr-826 phosphorylation of SSH1L in insulin-induced cofilin dephosphorylation, we analyzed the effects of expression of SSH1L(WT) or its T826A mutant. Expression of SSH1L(WT) or its T826A mutant markedly decreased the level of cofilin phosphorylation (Fig. 6*E*), suggesting that the cofilin phosphatase activity of SSH1L(T826A) is comparable with that of SSH1L(WT). Insulin stimulation further decreased the level of cofilin phosphorylation in both SSH1L(WT)- and SSH1L(T826A)-expressing cells (Fig. 6*E*), indicating that Thr-826 phosphorylation of SSH1L is not essential for insulin-induced cofilin dephosphorylation. Together with the finding that an Akt inhibitor VIII promoted cofilin dephosphorylation, these results suggest that Akt has the potential to phosphorylate SSH1L, but this phosphorylation is not involved in SSH1L activation and cofilin dephosphorylation.

Co-localization of IRS4 and SSH1L at Membrane Protrusions—To evaluate the cellular function of IRS4-SSH1L interaction, subcellular localization of these proteins was analyzed. When 293T cells were co-stained with an anti-IRS4 antibody and Alexa Fluor 568-labeled phalloidin, IRS4 was localized at the plasma membrane as reported previously (19), and it was concentrated and co-localized with F-actin near the plasma membrane (Fig. 7*A*). Insulin stimulation induced F-actin-rich membrane protrusions. IRS4 was enriched in these regions, whereas its distribution at the plasma membrane was not altered (Fig. 7*A*). To examine the subcellular localization of SSH1L and IRS4, 293T cells were transfected with Myc-SSH1L and co-stained with anti-Myc and anti-IRS4 antibodies. Both Myc-SSH1L and IRS4 were concentrated in the membrane protrusions in insulin-stimulated cells, whereas their co-localization was not evident in non-stimulated cells (Fig. 7*B*). In addition, to confirm that these protrusions are the site of the local activation of PI3K, localization of P-Akt (Ser-473) was assessed by immunostaining using an anti-P-Akt (Ser-473) antibody. Both IRS4 and SSH1L co-localized with P-Akt at the membrane protrusions in insulin-stimulated cells (Fig. 7, *C* and *D*). These observations suggest that active PI3K co-localizes with IRS4 and SSH1L in insulin-induced membrane protrusions.

DISCUSSION

In this study, we identified IRS4 as a novel SSH1-binding protein. Co-precipitation assays revealed that they associate endogenously, and immunostaining indicated that they co-localize in the F-actin-rich membrane protrusions in cultured cells. *In vitro* binding assays using purified IRS4 and SSH1L proteins revealed that they interact directly. We also showed that IRS4 binds to SSH1L primarily through a relatively smaller region (amino acids 335–400) adjacent to the C terminus of the PTB domain, whereas the C-terminal region (amino acids 1094–1257) has weak SSH1L binding ability. Both the PH and the PTB domains in the N-terminal region are highly conserved between the IRS family proteins, but the C-terminal region has little similarity. This could contribute to the selective binding of IRS4 to SSH1L among the different IRS isoforms. To date, the major SSH1L-binding region of IRS4 (amino acids 335–400) has not been assigned any functional role related to IRS4 and is not known to possess any functional domain or motif according to the available databases. In addition, this region does not contain phosphotyrosine or phosphoserine/-threonine motifs. Therefore, the findings of this study suggest that the region of amino acids 335–400 is a unique functional domain of IRS4 that is responsible for SSH1L binding.

We showed that the A, B, and P domains of SSH1L bind to IRS4 independently. However, in the combined state, the AB fragment lost its ability to bind to IRS4. This may be caused by the change in the conformation of the A and B domains by complex formation or by the reciprocal masking of the IRS4-binding sites in each domain. In addition, the binding of SSH1(N461) to IRS4 was weaker than that of the A, B, or P domain, and the binding of SSH1L to IRS4 was weaker than that of SSH1S. These results probably reflect the undetermined conformational states of each fragment and isoform of SSH1. Although the crystal structure of the P domain in SSH2 was

reported (20) and the B domain has a similarity to the DEK-C motif, further structural analyses of SSH1, IRS4, and their complex are required for better understanding of the binding characteristics in the interaction between IRS4 and SSH1.

Knockdown of IRS4 increased the level of cofilin phosphorylation, and overexpression of shRNA-resistant IRS4 reversed the increase in the level of cofilin phosphorylation induced by IRS4 knockdown. These results suggest that IRS4 promotes

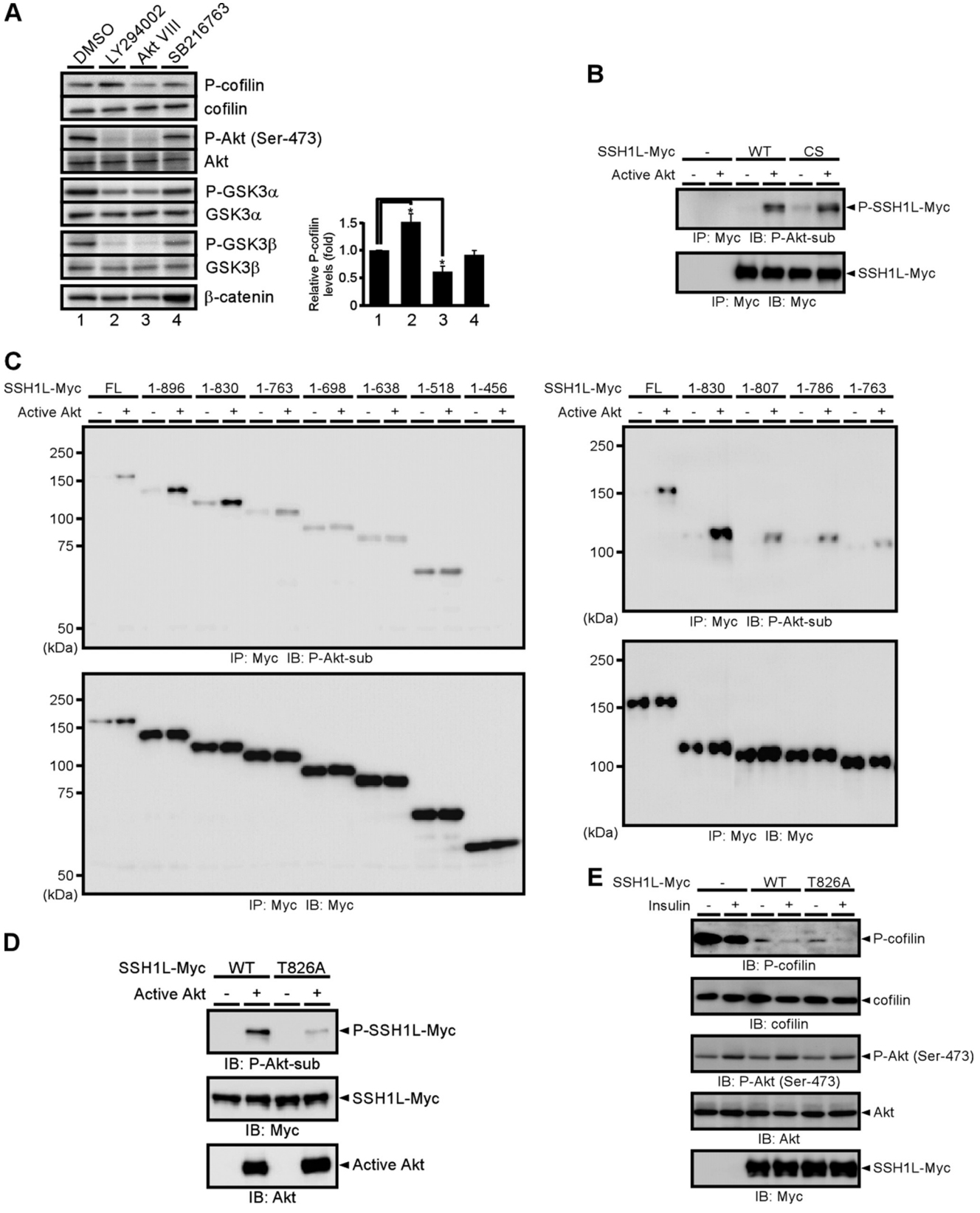

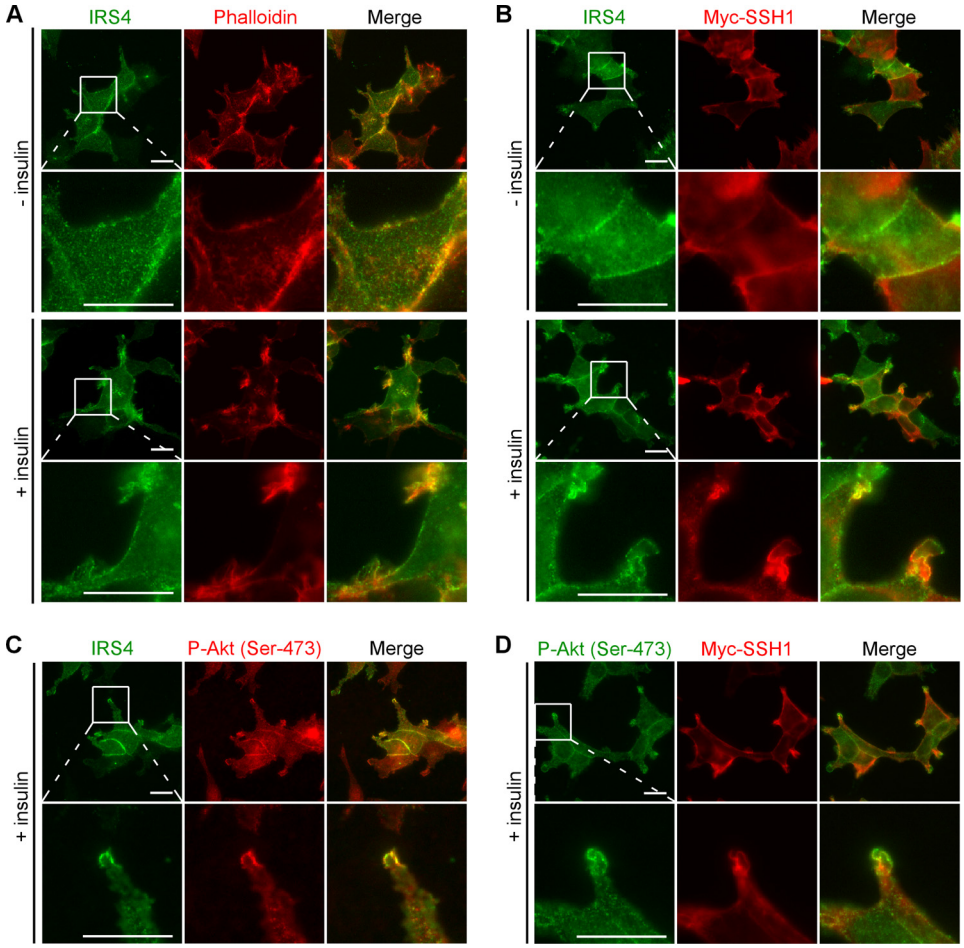

FIGURE 7. **Subcellular localization of IRS4 and SSH1.** *A*, localization of endogenous IRS4 in 293T cells. The 293T cells were plated on poly-L-lysine-coated coverslips, cultured for 24 h, and serum-starved for 2 h. Cells were treated with 1 μM insulin for 15 min or left untreated and fixed with formaldehyde followed by staining with an anti-IRS4 antibody (*green*) and Alexa Fluor 568-phalloidin for F-actin (*red*). Merged fluorescence images are shown in the *right panels*. Magnified images of the *white boxes* are shown in the *lower panels*. *B*, co-localization of IRS4 and SSH1L. The 293T cells were transfected with Myc-SSH1L and treated as in *A*. Cells were fixed and stained with anti-Myc (*red*) and anti-IRS4 antibodies (*green*). *C*, co-localization of IRS4 and P-Akt. The 293T cells were treated as in *A* and stained with anti-P-Akt (Ser-473) (*red*) and anti-IRS4 antibodies (*green*). *D*, co-localization of P-Akt and SSH1L. The 293T cells were treated as in *B*. Cells were stained with anti-Myc (*red*) and anti-P-Akt (Ser-473) antibodies (*green*). *Scale bars* in *A–D*, 20 μm.

cofilin dephosphorylation in cultured cells. However, *in vitro* phosphatase assays revealed that IRS4 has no direct effect on the cofilin phosphatase activity of SSH1L, which indicates that IRS4 promotes cofilin dephosphorylation by a mechanism that is different from the direct activation of SSH1L.

IRS family proteins are known to mediate insulin and growth factor signaling from the upstream tyrosine kinase receptors to the downstream signaling pathways, including activation of the PI3K-Akt pathway (15). Previous studies showed that overexpression of IRS4 induces higher levels of phosphatidylinositol 3,4,5-trisphosphate, Akt activation, and cell proliferation even in the absence of insulin or growth factors and that knockdown of IRS4 suppresses Akt activation and cell proliferation (21, 22). We also showed that knockdown of IRS4 reduced the levels of P-Akt (Thr-308 and Ser-473) and P-GSK3α/-3β and that expression of IRS4 restored the levels of these phosphoproteins in IRS4-depleted cells. These results suggest that endogenous IRS4 has the function to promote activation of the PI3K-Akt signaling pathway in 293T cells.

We have shown previously that SSH1L is activated downstream of PI3K (10). In accordance with this, LY294002, a specific inhibitor of PI3K, increased the level of cofilin phosphorylation, suggesting that PI3K promotes SSH1L activity and cofilin dephosphorylation. However, the mechanism by which

FIGURE 6. **Effects of inhibition of PI3K, Akt, and GSK3 on the level of cofilin phosphorylation and the role of Akt-mediated Thr-826 phosphorylation of SSH1L in insulin-induced cofilin dephosphorylation.** *A*, inhibition of PI3K, but not Akt or GSK3, increases cofilin phosphorylation. The 293T cells were treated with 20 μM LY294002, 10 μM Akt VIII, or 10 μM SB216763 for 2 h, and cell lysates were analyzed by immunoblotting as in Fig. 4. Inhibition of GSK3 was confirmed by the increased level of β-catenin. Quantification of the P-cofilin/cofilin ratio is shown on the *right*. Data are the means ± S.E. (*error bars*) ($n = 5$; unpaired *t* tests with Bonferroni correction). *, $p < 0.025$. *B–D*, Akt preferentially phosphorylates SSH1L at Thr-826. SSH1L-Myc or its mutants were expressed in 293T cells, immunoprecipitated (*IP*) with an anti-Myc antibody, and subjected to *in vitro* kinase assays using active Akt. CS, a SSH1L mutant with replacement of Cys-393 by Ser. Reaction mixtures were analyzed by immunoblotting (*IB*) with antibodies against phospho-Akt substrate (*sub*), Myc, and Akt. *E*, Thr-826 phosphorylation has no effect on cofilin phosphatase activity of SSH1L and insulin-induced cofilin dephosphorylation. The 293T cells were transfected with SSH1L (WT or T826A) or control vector, cultured for 24 h, serum-starved for 2 h, and then stimulated with 1 μM insulin for 20 min. Cell lysates were analyzed by immunoblotting with antibodies against P-cofilin, cofilin, P-Akt (Ser-473), Akt, and Myc.

PI3K activates SSH1L remains unknown. A recent study demonstrated that SSH2 is activated downstream of the Akt-GSK3 pathway (14). This study provided evidence that Akt inhibits the kinase activity of GSK3, which relieves GSK3-mediated phosphorylation and inhibition of SSH2, resulting in SSH2 activation and cofilin dephosphorylation (14). However, it has remained unknown whether SSH1L is activated through the Akt-GSK3 pathway in a way similar to that for SSH2. In this study, we showed that a PI3K inhibitor, but not an Akt inhibitor or a GSK3 inhibitor, increased the level of cofilin phosphorylation. Furthermore, Akt phosphorylated SSH1L at Thr-826, but the expression of the non-phosphorylatable T826A mutant of SSH1L had no apparent effect on either the cofilin phosphatase activity of SSH1L or the level of insulin-induced cofilin dephosphorylation. These results suggest that SSH1L is activated downstream of PI3K, but in contrast to the mechanism of SSH2 activation, SSH1L is not activated through the Akt-GSK3 pathway. Because PI3K also activates various downstream protein kinases, such as PDK1, PDK2, PKCζ, and mTOR (15), and Rac guanine nucleotide exchange factor P-Rex1 (23, 24), it is possible that SSH1L is activated downstream of PI3K through these signaling molecules.

In addition, the IRS4-SSH1L interaction may facilitate the localized activation of SSH1L at the membrane protrusions. SSH1L is a crucial factor in polarized cellular migration as it restricts the membrane protrusion to one direction and locally stimulates cofilin activity in the lamellipodium at the front of the migrating cell (11). Because IRS4 co-localizes with SSH1L in membrane protrusions in insulin-stimulated cells, IRS4 may play a role in the local activation of SSH1L by localizing SSH1L to the sites of its activation. Further studies will provide a better understanding of the cellular and physiological functions of IRS4 in the spatiotemporal regulation of SSH1L activity during cellular morphogenesis and migration.

IRS4 was identified as the fourth member of the IRS family proteins (25). IRS1 and IRS2 are expressed ubiquitously in the entire body, and knock-out of IRS1 or IRS2 in mice leads to severe phenotypes, such as marked growth retardation and diabetes, respectively (26–28). Conversely, IRS4 is expressed only in specific tissues, such as the thymus, pituitary gland, and hypothalamus (29–31), and cell lines, such as 293T, 293AAV, and HepG2 cells (22, 32). IRS4 knock-out mice exhibit mild defects in growth, reproduction, glucose homeostasis, and maternal behaviors (31, 33). Therefore, it is likely that IRS4 has more specialized cellular and physiological functions compared with IRS1 and IRS2. In addition to its unique expression pattern, its selective interaction with SSH1L may induce specialized cellular and physiological functions of IRS4 because other IRS isoforms, such as IRS1 and IRS2, do not bind to SSH1L.

REFERENCES

1. Bernstein, B. W., and Bamburg, J. R. (2010) ADF/cofilin: a functional node in cell biology. *Trends Cell Biol.* **20,** 187–195
2. Arber, S., Barbayannis, F. A., Hanser, H., Schneider, C., Stanyon, C. A., Bernard, O., and Caroni, P. (1998) Regulation of actin dynamics through phosphorylation of cofilin by LIM-kinase. *Nature* **393,** 805–809
3. Yang, N., Higuchi, O., Ohashi, K., Nagata, K., Wada, A., Kangawa, K., Nishida, E., and Mizuno, K. (1998) Cofilin phosphorylation by LIM-kinase 1 and its role in Rac-mediated actin reorganization. *Nature* **393,** 809–812
4. Toshima, J., Toshima, J. Y., Amano, T., Yang, N., Narumiya, S., and Mizuno, K. (2001) Cofilin phosphorylation by protein kinase TESK1 and its role in integrin-mediated actin reorganization and focal adhesion formation. *Mol. Biol. Cell* **12,** 1131–1145
5. Mizuno, K. (2013) Signaling mechanisms and functional roles of cofilin phosphorylation and dephosphorylation. *Cell. Signal.* **25,** 457–469
6. Niwa, R., Nagata-Ohashi, K., Takeichi, M., Mizuno, K., and Uemura, T. (2002) Control of actin reorganization by Slingshot, a family of phosphatases that dephosphorylate ADF/cofilin. *Cell* **108,** 233–246
7. Ohta, Y., Kousaka, K., Nagata-Ohashi, K., Ohashi, K., Muramoto, A., Shima, Y., Niwa, R., Uemura, T., and Mizuno, K. (2003) Differential activities, subcellular distribution and tissue expression patterns of three members of Slingshot family phosphatases that dephosphorylate cofilin. *Genes Cells* **8,** 811–824
8. Gohla, A., Birkenfeld, J., and Bokoch, G. M. (2005) Chronophin, a novel HAD-type serine protein phosphatase, regulates cofilin-dependent actin dynamics. *Nat. Cell Biol.* **7,** 21–29
9. Nagata-Ohashi, K., Ohta, Y., Goto, K., Chiba, S., Mori, R., Nishita, M., Ohashi, K., Kousaka, K., Iwamatsu, A., Niwa, R., Uemura, T., and Mizuno, K. (2004) A pathway of neuregulin-induced activation of cofilin-phosphatase Slingshot and cofilin in lamellipodia. *J. Cell Biol.* **165,** 465–471
10. Nishita, M., Wang, Y., Tomizawa, C., Suzuki, A., Niwa, R., Uemura, T., and Mizuno, K. (2004) Phosphoinositide 3-kinase-mediated activation of cofilin phosphatase Slingshot and its role for insulin-induced membrane protrusion. *J. Biol. Chem.* **279,** 7193–7198
11. Nishita, M., Tomizawa, C., Yamamoto, M., Horita, Y., Ohashi, K., and Mizuno, K. (2005) Spatial and temporal regulation of cofilin activity by LIM kinase and Slingshot is critical for directional cell migration. *J. Cell Biol.* **171,** 349–359
12. Wang, Y., Shibasaki, F., and Mizuno, K. (2005) Calcium signal-induced cofilin dephosphorylation is mediated by Slingshot via calcineurin. *J. Biol. Chem.* **280,** 12683–12689
13. Kurita, S., Watanabe, Y., Gunji, E., Ohashi, K., and Mizuno, K. (2008) Molecular dissection of the mechanisms of substrate recognition and F-actin-mediated activation of cofilin-phosphatase Slingshot-1. *J. Biol. Chem.* **283,** 32542–32552
14. Tang, W., Zhang, Y., Xu, W., Harden, T. K., Sondek, J., Sun, L., Li, L., and Wu, D. (2011) A PLCβ/PI3Kγ-GSK3 signaling pathway regulates cofilin phosphatase slingshot2 and neutrophil polarization and chemotaxis. *Dev. Cell* **21,** 1038–1050
15. White, M. F. (2002) IRS proteins and the common path to diabetes. *Am. J. Physiol. Endocrinol. Metab.* **283,** E413–E422
16. Kaji, N., Ohashi, K., Shuin, M., Niwa, R., Uemura, T., and Mizuno, K. (2003) Cell cycle-associated changes in Slingshot phosphatase activity and roles in cytokinesis in animal cells. *J. Biol. Chem.* **278,** 33450–33455
17. Ogihara, T., Isobe, T., Ichimura, T., Taoka, M., Funaki, M., Sakoda, H., Onishi, Y., Inukai, K., Anai, M., Fukushima, Y., Kikuchi, M., Yazaki, Y., Oka, Y., and Asano, T. (1997) 14-3-3 protein binds to insulin receptor substrate-1, one of the binding sites of which is in the phosphotyrosine binding domain. *J. Biol. Chem.* **272,** 25267–25274
18. Hong, Z., Jiang, J., Lan, L., Nakajima, S., Kanno, S., Koseki, H., and Yasui, A. (2008) A polycomb group protein, PHF1, is involved in the response to DNA double-strand breaks in human cell. *Nucleic Acids Res.* **36,** 2939–2947
19. Fantin, V. R., Sparling, J. D., Slot, J. W., Keller, S. R., Lienhard, G. E., and Lavan, B. E. (1998) Characterization of insulin receptor substrate 4 in human embryonic kidney 293 cells. *J. Biol. Chem.* **273,** 10726–10732
20. Jung, S. K., Jeong, D. G., Yoon, T. S., Kim, J. H., Ryu, S. E., and Kim, S. J. (2007) Crystal structure of human slingshot phosphatase 2. *Proteins* **68,** 408–412
21. Shimwell, N. J., Martin, A., Bruton, R. K., Blackford, A. N., Sedgwick, G. G., Gallimore, P. H., Turnell, A. S., and Grand, R. J. (2009) Adenovirus 5 E1A is responsible for increased expression of insulin receptor substrate 4 in established adenovirus 5-transformed cell lines and interacts with IRS components activating the PI3 kinase/Akt signalling pathway. *Oncogene* **28,** 686–697
22. Hoxhaj, G., Dissanayake, K., and MacKintosh, C. (2013) Effect of IRS4 levels on PI 3-kinase signalling. *PLoS One* **8,** e73327

23. Sosa, M. S., Lopez-Haber, C., Yang, C., Wang, H., Lemmon, M. A., Busillo, J. M., Luo, J., Benovic, J. L., Klein-Szanto, A., Yagi, H., Gutkind, J. S., Parsons, R. E., and Kazanietz, M. G. (2010) Identification of the Rac-GEF P-Rex1 as an essential mediator of ErbB signaling in breast cancer. *Mol. Cell* **40,** 877–892
24. Wertheimer, E., Gutierrez-Uzquiza, A., Rosemblit, C., Lopez-Haber, C., Sosa, M. S., and Kazanietz, M. G. (2012) Rac signaling in breast cancer: a tale of GEFs and GAPs. *Cell. Signal.* **24,** 353–362
25. Lavan, B. E., Fantin, V. R., Chang, E. T., Lane, W. S., Keller, S. R., and Lienhard, G. E. (1997) A novel 160-kDa phosphotyrosine protein in insulin-treated embryonic kidney cells is a new member of the insulin receptor substrate family. *J. Biol. Chem.* **272,** 21403–21407
26. Araki, E., Lipes, M. A., Patti, M. E., Brüning, J. C., Haag, B., 3rd, Johnson, R. S., and Kahn, C. R. (1994) Alternative pathway of insulin signalling in mice with targeted disruption of the IRS-1 gene. *Nature* **372,** 186–190
27. Tamemoto, H., Kadowaki, T., Tobe, K., Yagi, T., Sakura, H., Hayakawa, T., Terauchi, Y., Ueki, K., Kaburagi, Y., and Satoh, S. (1994) Insulin resistance and growth retardation in mice lacking insulin receptor substrate-1. *Nature* **372,** 182–186
28. Withers, D. J., Gutierrez, J. S., Towery, H., Burks, D. J., Ren, J. M., Previs, S., Zhang, Y., Bernal, D., Pons, S., Shulman, G. I., Bonner-Weir, S., and White, M. F. (1998) Disruption of IRS-2 causes type 2 diabetes in mice. *Nature* **391,** 900–904
29. Numan, S., and Russell, D. S. (1999) Discrete expression of insulin receptor substrate-4 mRNA in adult rat brain. *Brain Res. Mol. Brain Res.* **72,** 97–102
30. Uchida, T., Myers, M. G., Jr., and White, M. F. (2000) IRS-4 mediates protein kinase B signaling during insulin stimulation without promoting antiapoptosis. *Mol. Cell. Biol.* **20,** 126–138
31. Xu, X., Coats, J. K., Yang, C. F., Wang, A., Ahmed, O. M., Alvarado, M., Izumi, T., and Shah, N. M. (2012) Modular genetic control of sexually dimorphic behaviors. *Cell* **148,** 596–607
32. Cuevas, E. P., Escribano, O., Chiloeches, A., Ramirez Rubio, S., Román, I. D., Fernández-Moreno, M. D., and Guijarro, L. G. (2007) Role of insulin receptor substrate-4 in IGF-I-stimulated HEPG2 proliferation. *J. Hepatol.* **46,** 1089–1098
33. Fantin, V. R., Wang, Q., Lienhard, G. E., and Keller, S. R. (2000) Mice lacking insulin receptor substrate 4 exhibit mild defects in growth, reproduction, and glucose homeostasis. *Am. J. Physiol. Endocrinol. Metab.* **278,** E127–E133